The Nitric Oxide/Cyclic GMP Pathway in the Olfactory Processing System of the Terrestrial Slug Limax marginatus

Authors: Fujie, Sayoko, Aonuma, Hitoshi, Ito, Iori, Gelperin, Alan, and Ito, Etsuro

Source: Zoological Science, 19(1) : 15-26

Published By: Zoological Society of Japan

URL: https://doi.org/10.2108/zsj.19.15

ZOOLOGICAL SCIENCE **19**: 15–26 (2002)

The Nitric Oxide/Cyclic GMP Pathway in the Olfactory Processing System of the Terrestrial Slug *Limax marginatus*

Sayoko Fujie[1], Hitoshi Aonuma[2], Iori Ito[1], Alan Gelperin[3] and Etsuro Ito[1]*

[1]*Laboratory of Animal Behavior and Intelligence, Division of Biological Sciences, Graduate School of Science, Hokkaido University, Sapporo 060-0810, Japan*
[2]*Laboratory of Neuro-Cybernetics, Research Institute for Electronic Science, Hokkaido University, Sapporo 060-0812, Japan*
[3]*Monell Chemical Senses Center, Philadelphia, PA 19104, USA*

ABSTRACT—To examine the distribution of nitric oxide (NO)-generative cells and NO-responsive cells in the tentacles and procerebral lobes (olfactory processing center) of terrestrial slugs, we applied NADPH diaphorase (NADPH-d) histochemistry and NO-induced cyclic GMP (cGMP)-like immunohistochemistry. We found that NADPH-d reactive cells/fibers and cGMP-like immunoreactive cells/fibers were different, but they were localized adjacent to each other, in both the tentacles and the procerebral lobes. Then, we measured the concentration of NO that was generated around the procerebral lobes using an NO sensitive electrode, when the olfactory nerve was electrically stimulated as a replacement for an odorant stimulus. Stimulation of the olfactory nerve evoked an increase in NO concentration at nanomolar levels, suggesting that binding of nanomolar concentrations of NO to the prosthetic heme group activates soluble guanylyl cyclase. Taken together with previously reported physiological data, our results, therefore, showed that the NO/cGMP pathways are involved in slug olfactory processing.

Key words: gaseous signaling molecule, mollusk, NADPH-diaphorase histochemistury, NO measurement, procerebral lobe

INTRODUCTION

Nitric oxide (NO) is an unconventional neurotransmitter because it diffuses easily from its production site through cell membranes and moves readily through the brain in three dimensions (Sadamoto *et al*., 1998; Kobayashi *et al*., 2000a, b; Philippides *et al*., 2000). NO is generated by catalysis of nitric oxide synthase (NOS), which employs L-arginine, O_2, and NADPH-derived electrons (Marletta *et al*., 1988). This indicates that formation of NO requires the presence of NADPH as a cofactor of NOS. Therefore a simple histochemical method to localize NOS-containing cells is to stain fixed nervous tissues for NADPH diaphorase (NADPH-d) (Gelperin, 1994a; Sadamoto *et al*., 1998; Gelperin *et al*., 2000, 2001). The principle function of NO in many systems is to activate soluble guanylyl cyclase, resulting in production of cyclic GMP (cGMP), which can act on cGMP-activated protein kinase to phosphorylate downstream target proteins and thus evoke cellular responses (Bredt and Snyder, 1992; Garthwaite and Boulton, 1995; Aonuma *et al*., 2000, Aonuma and Newland, 2001; Bicker, 2001).

Many lines of evidence indicate that NO plays important roles in olfactory processing as seen in both invertebrates and vertebrates (Breer and Shepherd, 1993; Gelperin, 1994a, b, 1999; Robertson *et al*., 1994, 1995; Müller and Hildebrandt, 1995; Gelperin *et al*., 1996, 2000, 2001; Müller, 1996; Okere *et al*., 1996, Teyke, 1996; Hildebrand and Shepherd, 1997; Kendrick *et al*., 1997; Koh and Jacklet, 1999; Teyke and Gelperin, 1999; Moroz, 2001). Previous observations suggested that NO-mediated signaling in olfactory systems operates in parallel with conventional synaptic transmission to synchronize the neural activity. For example, field potential oscillations, thought to underlie synchrony of odor-responding interneurons, are dependent on NO levels in the olfactory system of the terrestrial slug *Limax maximus* (Gelperin, 1994a, b, 1999; Gelperin *et al*., 1996, 2000, 2001; Teyke and Gelperin, 1999). The olfactory processing center, the procerebral lobe, of slugs has a relatively simple, regular structure and displays robust spontaneous oscillations, offering many advantages for understanding the functional roles of synchronized neural activity for olfactory processing (Kleinfeld *et al*., 1994; Gervais *et al*., 1996; Ermentrout *et al*., 1998, 2001; Ito *et al*., 1999, 2001; Teyke *et al*., 1999;

* Corresponding author: Tel. +81-11-706-2615;
FAX. +81-11-706-4448.
E-mail: eito@sci.hokudai.ac.jp

Cooke and Gelperin, 2001; Wang *et al*., 2001). Despite the fact that NO signaling and synchronized neural activity appear to be characteristic for olfactory processing in slugs (Gelperin, 1994a, b, 1999; Gelperin *et al*., 1996, 2000, 2001; Teyke and Gelperin, 1999), the detailed cellular pathways of NO/cGMP signaling remain to be examined with histological techniques.

In the present study, we applied NADPH-d histochemistry and NO-induced cGMP-like immunohistochemistry to examine the distribution of NO-generative cells and NO-responsive cells, respectively, in the tentacles and procerebral lobes of the terrestrial slug *L. marginatus*. Then, we measured the concentration of NO that is generated around the procerebral lobes using an NO sensitive electrode, when the olfactory nerve was electrically stimulated as a replacement for an odorant stimulus. We found that NADPH-d reactive cells/fibers and cGMP-like immunoreactive cells/fibers were different, but adjacent to each other, in both the tentacles and the central nervous system (CNS). The NO measurements showed that stimulation of the olfactory input pathway evoked an increase in NO concentration at nanomolar levels, suggesting that binding of nanomolar concentrations of NO to the prosthetic heme group activates soluble guanylyl cyclase.

MATERIALS AND METHODS

Slugs

Adult specimens of the terrestrial slug *L. marginatus* weighing 0.5-1.5 g were used. Slugs were obtained from our laboratory colony or collected in the open field, maintained in our laboratory in a 14:10 h light:dark cycle at 19°C and fed on a paste of rat chow. Slugs were anesthetized by injection of 0.2-0.3 ml of an anesthetizing solution (see Ito *et al*., 1999 for composition) before dissection.

NADPH diaphorase histochemistry on whole mount preparations and cryostat-section preparations

The entire CNS together with the tentacles was removed from anesthetized slugs. For whole mount preparations, these tissues were fixed with 3.7% formaldehyde for 20 min at 4°C, rinsed twice in 0.1 M Tris-HCl (pH 8.0) with 0.2% Triton X-100 for 20 min at 4°C, incubated with a staining solution (0.2 mM β-NADPH (tetrasodium; Sigma, St. Louis, MO), 0.2 mM nitro blue tetrazolium (NBT, Sigma), and 0.2% Triton X-100 in 0.1 M Tris-HCl (pH 8.0)) overnight at 4°C, washed twice in distilled water for 10 min at room temperature, post-fixed in methanol and acetic acid (3:1) for 30 min, dehydrated in 100% methanol for 40 min, and cleared in cedarwood oil (Biken, Tokyo, Japan) for 10 min. The preparations were examined under a light microscope (MICROPHOTO-FXA; Nikon, Tokyo, Japan). To prepare cryostat-sections, the tissues were fixed with 4% paraformaldehyde in phosphate buffer (PB, pH 7.6) for 1 hr at 4°C, cryo-protected in 30% sucrose in PB overnight at 4°C, embedded in Tissue-Tek O.C.T. compound (Sakura Finetek, Torrance, CA), and sectioned with a cryostat (CM 3000; Leica, Nossloch, Germany) at a thickness of 20 μm. The sections were collected on silane-coated slides (Muto Pure Chemicals, Tokyo, Japan), air-dried at room temperature, rinsed three times in 0.1 M Tris-HCl (pH 8.0) for 15 min, incubated with the staining solution for 1 hr, washed in distilled water, and mounted in glycerol (Nakarai, Kyoto, Japan). The cryostat sections were also examined under a light microscope.

Cyclic GMP-like immunohistochemistry on cryostat-sectioned preparations

Staining methods were modified from Ott *et al*. (2000). The entire CNS together with the tentacles was removed from anesthetized slugs. The cerebral commissure was cut to facilitate penetration of reagents. For detection of NO-induced cGMP responses, the tissues were first incubated with 1 mM 3-isobutyl-1-methyxanthine (IBMX; Sigma) in *Limax* saline (see Ito *et al*., 1999 for composition) for 30 min at 4°C, and then they were incubated with 20 mM sodium nitroprusside (SNP; Wako Pure Chemical Industries, Osaka, Japan) and 1 mM IBMX in *Limax* saline for 15 min at room temperature. IBMX is an endogenous phosphodiesterase inhibitor and SNP is an NO-generative agent, respectively. The tissues were fixed with 4% paraformaldehyde in 0.1 M PB (pH 7.6) overnight at 4°C, cryo-protected with 30% sucrose in PB, embedded in Tissue-Tek O.C.T. compound, and sectioned with a cryostat at a thickness of 20 μm. The sections were collected on silane-coated slides, air-dried at room temperature, rinsed three times in 0.1 M PBS (pH 7.4) with 0.2% Triton X-100 for 15 min, and incubated with 5% normal donkey serum in 0.1 M PBS with 0.2% Triton X-100 for 2 hr at room temperature. The preparations were incubated with primary antibody (sheep anti-cGMP antiserum, diluted 1:20000 in 0.1 M PBS with 0.2% Triton X-100 and 5% donkey serum) overnight at 4°C. The antiserum was a gift from Dr. Jan De Vente (Rijksuniversiteit Limburg, The Netherlands, see Tanaka *et al*., 1997 for its specificity and characterization). They were washed in 0.1 M PBS with 0.2% Triton X-100 and incubated with horseradish peroxidase-conjugated secondary anti-sheep IgG antibody (diluted 1:500 in 0.1 M PBS with 0.2% Triton X-100 and 5% donkey serum; Jackson ImmunoResearch Laboratories, West Grove, PA) for 2–3 hr at room temperature. After the development of staining with diaminobenzidine, secntions were washed in distilled water, dehydrated in an ethanol series, cleared in xylene, and mounted in Bioleit (Takaken, Tokyo, Japan). The preparations were examined under a light microscope. Control preparations were not incubated in IBMX or SNP.

Double staining for NADPH diaphorase and cyclic GMP on cryostat-sectioned preparations

Double staining methods were performed according to Bicker *et al*. (1996, 1997). The binding of the cGMP antiserum was first detected by immunohistochemistry and then the staining for NADPH-d was done subsequently by histochemistry on the same cryostat-section preparations. The exceptions from the above methods are as follows. The CNS and tentacles were fixed with a 4% paraformaldehyde solution for 2 hr. For the subsequent visualization of NADPH-d reactivity, the preparations were washed in 0.1 M PBS with 0.2% Triton X-100, and incubated with the staining solution for 30 min. They were finally mounted in glycerol.

Electron microscopy

Superior tentacles were clipped at the base from the bodies of anesthetized slugs with a pair of fine scissors. They were fixed with 1% paraformaldehyde and 1% gluteraldehyde in 0.1 M PB (pH 7.6) for 30 min at room temperature, rinsed three times in PB, and post-fixed with 1% osmium tetroxide in distilled water for 1 hr at 4°C. The fixed preparations were then dehydrated in an ethanol series and embedded in Luft's epon embedding medium according to a standard method. The embedded preparations were cut horizontally with a diamond knife (*Diatome* ultra 45°; Diatome, Biel, Switzerland) on an ultramicrotome (Porter-Blum MT-1; Ivan Sorvall, Newtown, CT), and stained by uranyl acetate for 9 min and by lead citrate for 3 min at room temperature. The stained ultrathin sections were observed under a transmission electron microscope (JEM-100S; JEOL, Tokyo, Japan).

NO measurement

The methods for NO measurement were modified from Koba-

yashi *et al*. (2000a, b). NO concentration was measured with an NO meter (ISO-NO; World Precision Instruments, Sarasota, FL) using an NO electrode with a tip diameter of 100 μm (ami-NO100; Innovative Instruments, Tampa, FL). The NO meter was provided by courtesy of World Precision Instruments Japan. The specificity of the NO measurement methods has previously been determined by Weyrich *et al*. (1994) and Kobayashi *et al*. (2000b). In addition, we examined the selectivity of the NO electrode. Sensitivity for NO_2^- and NO_3^- was tested by applying KNO_2 and KNO_3 (1 mM each) several times to the NO electrode in HEPES-buffered saline (pH 7.6). Dopamine, acetylcholine (1 mM each), and serotonin (0.5 mM), all electrically active monoamines associated with activation of olfactory signal transduction, were also applied to the NO electrode in HEPES-buffered saline. Furthermore, we tested the NO electrode response to pH changes (pH 4.0, 7.0, and 9.0).

The CNS and the superior tentacular nerves, that project to the procerebral lobes in the CNS, were dissected from anesthetized slugs and maintained in a Sylgard-coated recording dish perfused with *Limax* saline. The tip of the NO electrode was placed on the ventral surface of the internal mass from which the outer ganglionic sheath had been removed. NO signals recorded by the NO meter were monitored with an oscilloscope, and recorded with a computer. We set a criterion level of response such that responses over the noise level could be clearly distinguished as due to nerve stimulation. To remove NO from the recording dish, an NO scavenger, 2-phenyl-4, 4, 5, 5-tetramethylimidazoline-1-oxyl-3-oxide (PTIO, 1 mM; Sigma) was applied in *Limax* saline. A 3 sec pulse of 10 μA current was delivered to the superior tentacular nerve end, ipsilateral to the recording region of procerebral lobe, by a suction electrode made of a syringe body and a polyvinylchloride tip whose diameter (ca. 200 μm) was adjusted to fit the nerve cross-section. This method of electrical stimulation was used as a replacement for the odorant stimulus because it could be readily controlled in both time and amplitude.

The NO electrode was calibrated by decomposition of an NO-generative agent, *S*-nitroso-*N*-acetylpenicillamine (SNAP; Dojindo, Kumamoto, Japan), according to the Instruction Manual of World Precision Instruments (Sarasota, FL). Although the theoretical concentration of generated NO should be equal to the final concentration of SNAP in the calibration vial, the practical conversion ratio of SNAP to NO is approximately 53.9% (Askew *et al*., 1995). We therefore took this ratio into account for the calibration. Briefly, 1.3 mg SNAP was first dissolved in 50 ml of 0.02% EDTA (pH 9.0). Then, this SNAP solution was gradually added to 0.1 M copper sulfate in distilled water (pH 4.0) to generate NO at concentrations of 0, 2.2, 4.4, 6.6, 8.7, 10.9, 13.4, 22.0, 32.8, 43.5, 65.1, 87.0, and 109 nM. SNAP decomposes to NO and a disulfide byproduct in the presence of copper sulfate as a catalyst. The calibration was performed before and after NO measurements in tissue.

Statistical analysis

Statistical significance was examined by two-factor factorial ANOVA for the NO electrode calibration.

RESULTS

NADPH diaphorase histochemistry in the superior and inferior tentacles

When the whole mount preparations were examined, the tentacular ganglia had strong reactivity for NADPH-d (Fig. 1a). This evidence was supported by the control experiments in which the preparations made without application of NADPH did not show this reactivity (Fig. 1a). The NADPH-d reactivity was observed in both the superior and inferior tentacular ganglia and there were no differences in the staining pattern between these two tentacles. To investigate the details of NADPH-d reactivity, we prepared cryostat sections. The NADPH-d reactivity was found throughout the tentacular ganglia and in some cells underneath the sensory epithelia (Fig. 1b). These details were the same in both the superior and inferior tentacles. The NADPH-d reactivity in sensory neurons underneath the sensory epithelia was localized in cytoplasm in the cell bodies (Fig. 1c). The dendrites of these neurons were confirmed to extend to the sensory epithelia. Two types of interneurons, monopolar and bipolar ones, were stained by NADPH-d as well, both of which were located between the sensory epithelia and the tentacular ganglia (Fig. 1d, e; see Ito *et al*., 2000 for identification of cells). The collar cells were identified around the surfaces of the tentacular ganglia (see Hatakeyama *et al*., 2001 for details) and some of them were stained by NADPH-d (Fig. 1f).

Cyclic GMP-like immunohistochemistry in the superior and inferior tentacles

From low-power views of cryostat-section preparations, we observed strong cGMP-like immunoreactivity in the tentacular ganglia, which were incubated in IBMX (phosphodiesterase inhibitor) and SNP (NO generating agent) (Fig. 2a). This immunoreactivity was eliminated when both IBMX and SNP were omitted during incubation (Fig. 2a). Control preparations without application of antiserum against cGMP had no signals, either (data not shown). The staining pattern by cGMP antibody was the same in the superior and inferior tentacles. Two subtypes of interneurons were stained between the sensory epithelia and the tentacular ganglia. One was a monopolar interneuron (Fig. 2b), and the other was a bipolar one (Fig. 2c; see Ito *et al*., 2000). In the tentacular ganglia, some stained fibers were located near the tentacular nerves (Fig. 2d). The immunoreactive cells on the lateral surfaces of the tentacular ganglia formed lines (Fig. 2e). Near these immunoreactive cells, the immunoreactive fibers were assembled (Fig. 2e). In the regions of tentacular ganglia near the digits, some immunoreactive spots (2–3 μm in diameter) forming lines were found (Fig. 2f). We could not identify whether they were glial cells or cut ends of fibers.

Double staining for NADPH diaphorase and cyclic GMP in the superior and inferior tentacles

In some cryostat-section preparations, strongly immunoreactive regions recognized by cGMP antibody were found in the tentacular ganglia, whereas those structures stained by NADPH-d were found as fibers in the tentacular nerves (Fig. 3a). These fibers projected to the procerebral lobes. In other preparations, strongly cGMP-like immunoreactive fibers were also found to project to the procerebral lobes through the tentacular ganglia and the tentacular nerves (Fig. 3b). As far as we observed, the NADPH-d reactive fibers and the cGMP-like immunoreactive ones were completely different. The NADPH-d stained fibers in the

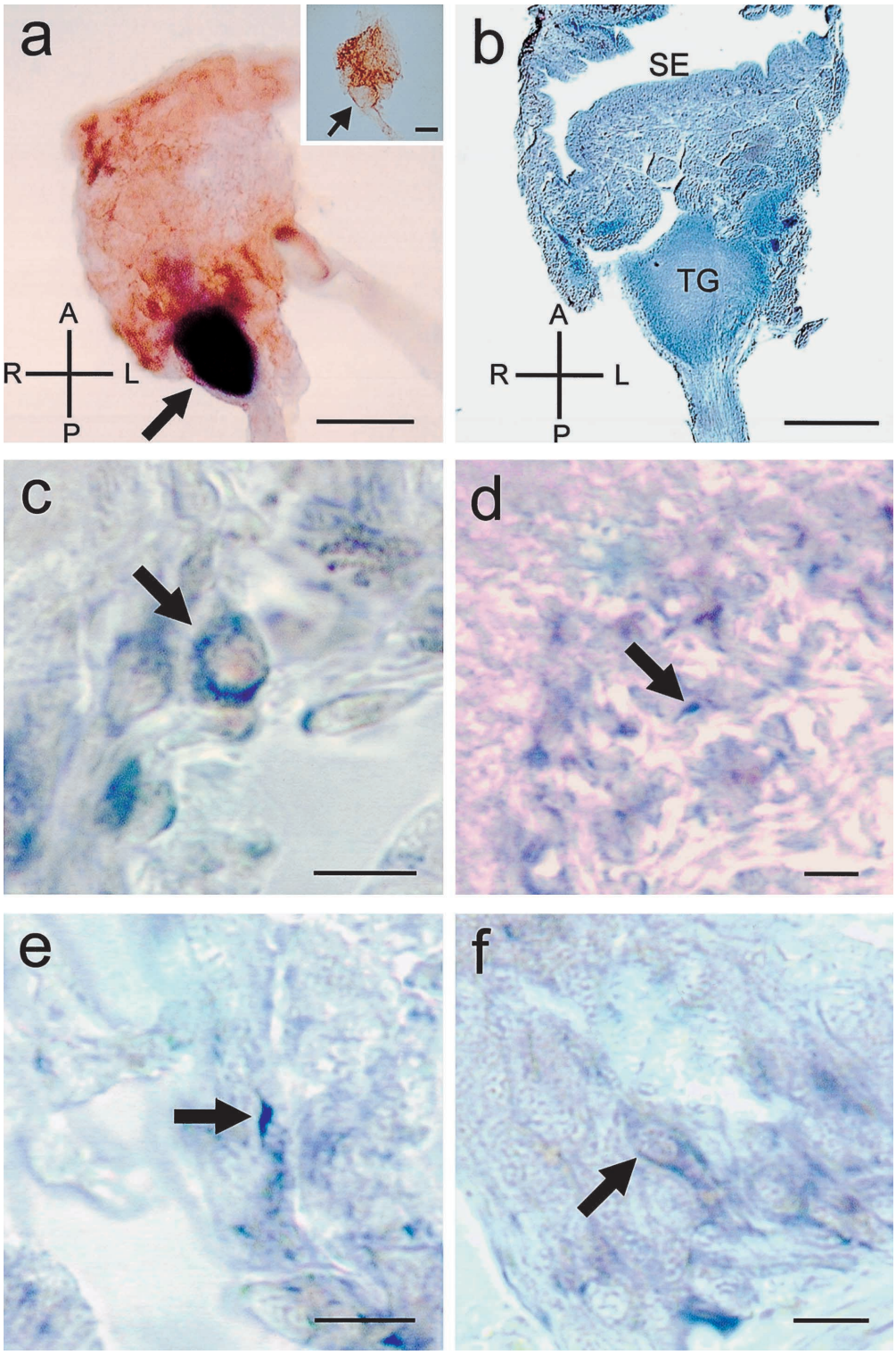

Fig. 1. NADPH diaphorase histochemistry in superior and inferior tentacles viewed from the ventral side. Note that NADPH-d signals are deep blue and that there were no differences in the staining pattern between the superior and inferior tentacles. (a) A whole mount preparation of an inferior tentacle. Arrow points to the tentacular ganglion. Inset shows a control preparation without application of NADPH. Scale bars, 150 μm. A; anterior, P; posterior, L; left, R; right. (b) A whole view of a superior tentacle in a cryostat-section preparation. SE; sensory epithelium, TG; tentacular ganglion. Scale bar, 200 μm. (c) A sensory neuron, pointed by an arrow, underneath the SE in a superior tentacle in a cryostat-section preparation. Scale bar, 10 μm. (d) A monopolar interneuron, pointed by an arrow, between the SE and TG in a superior tentacle in a cryostat-section preparation. Scale bar, 10 μm. (e) A bipolar interneuron, pointed by an arrow, between the SE and TG in an inferior tentacle in a cryostat-section preparation. Scale bar, 10 μm. (f) A collar cell, pointed by an arrow, in a superior tentacle in a cryostat-section preparation. Scale bar, 10 μm.

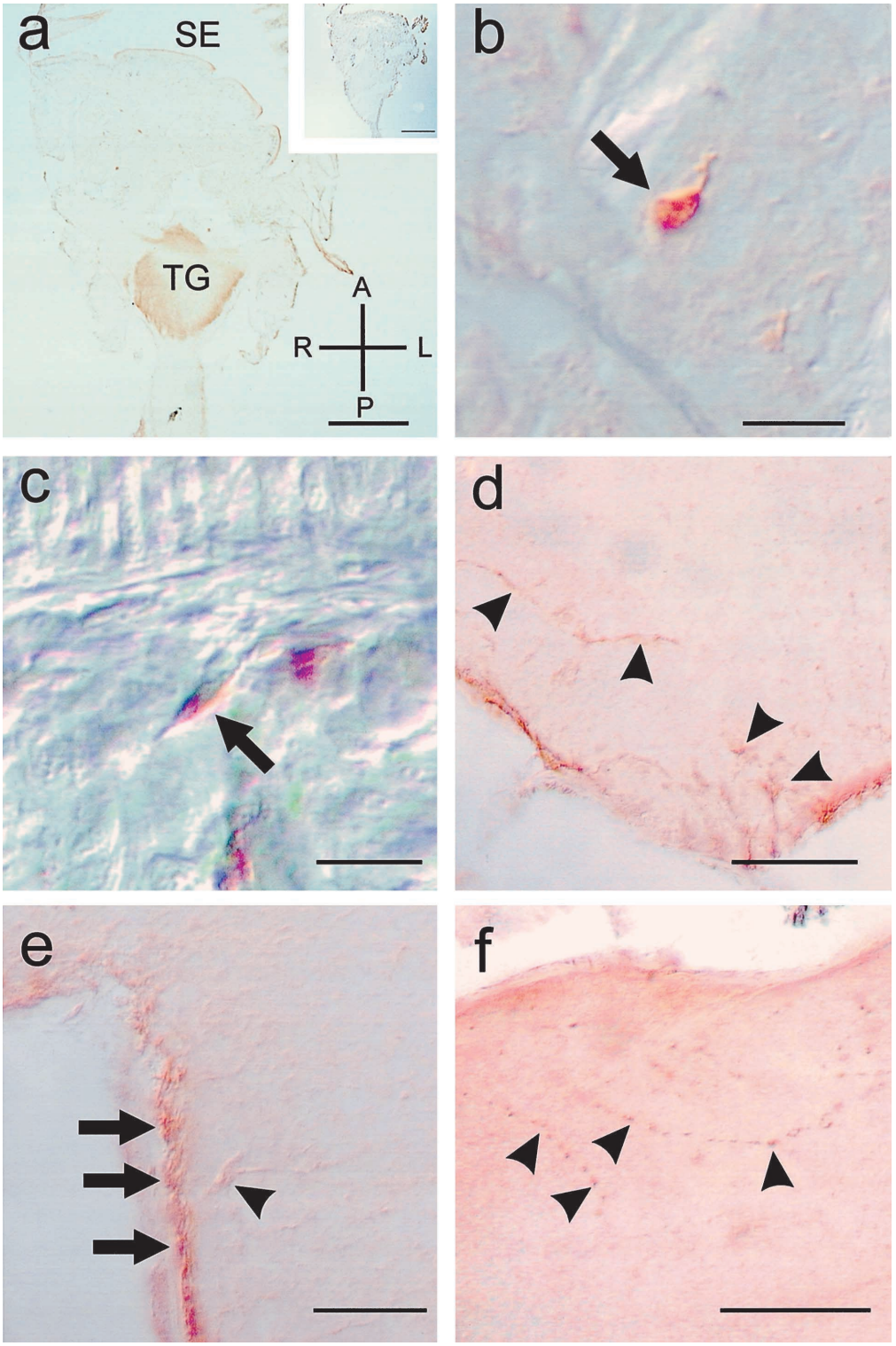

Fig. 2. Cyclic GMP-like immunohistochemistry in superior and inferior tentacles in cryostat-section preparations viewed from the ventral side. Note that cGMP-like immunoreactive signals are brown and that there were no differences in the staining pattern between the superior and inferior tentacles. (a) A whole view of a superior tentacle. SE; sensory epithelium, TG; tentacular ganglion. Inset shows a control preparation without application of IBMX and SNP. Scale bars, 200 μm. A; anterior, P; posterior, L; left, R; right. (b) A monopolar interneuron, pointed by an arrow, between the SE and TG in an inferior tentacle. Scale bar, 10 μm. (c) A bipolar interneuron, pointed by an arrow, between the SE and TG in an inferior tentacle. Scale bar, 10 μm. (d) Fibers, pointed by arrowheads, in the TG in an inferior tentacle. These fibers were located near the tentacular nerves. Scale bar, 50 μm. (e) A line of cell bodies (arrows) on the lateral surface of the TG in an inferior tentacle. An arrowhead points to fibers assembled near the immunoreactive cells. Scale bar, 30 μm. (f) Some spots forming lines, indicated by arrowheads, in the upper region of TG in a superior tentacle. These spots were near the digits. Scale bar, 50 μm.

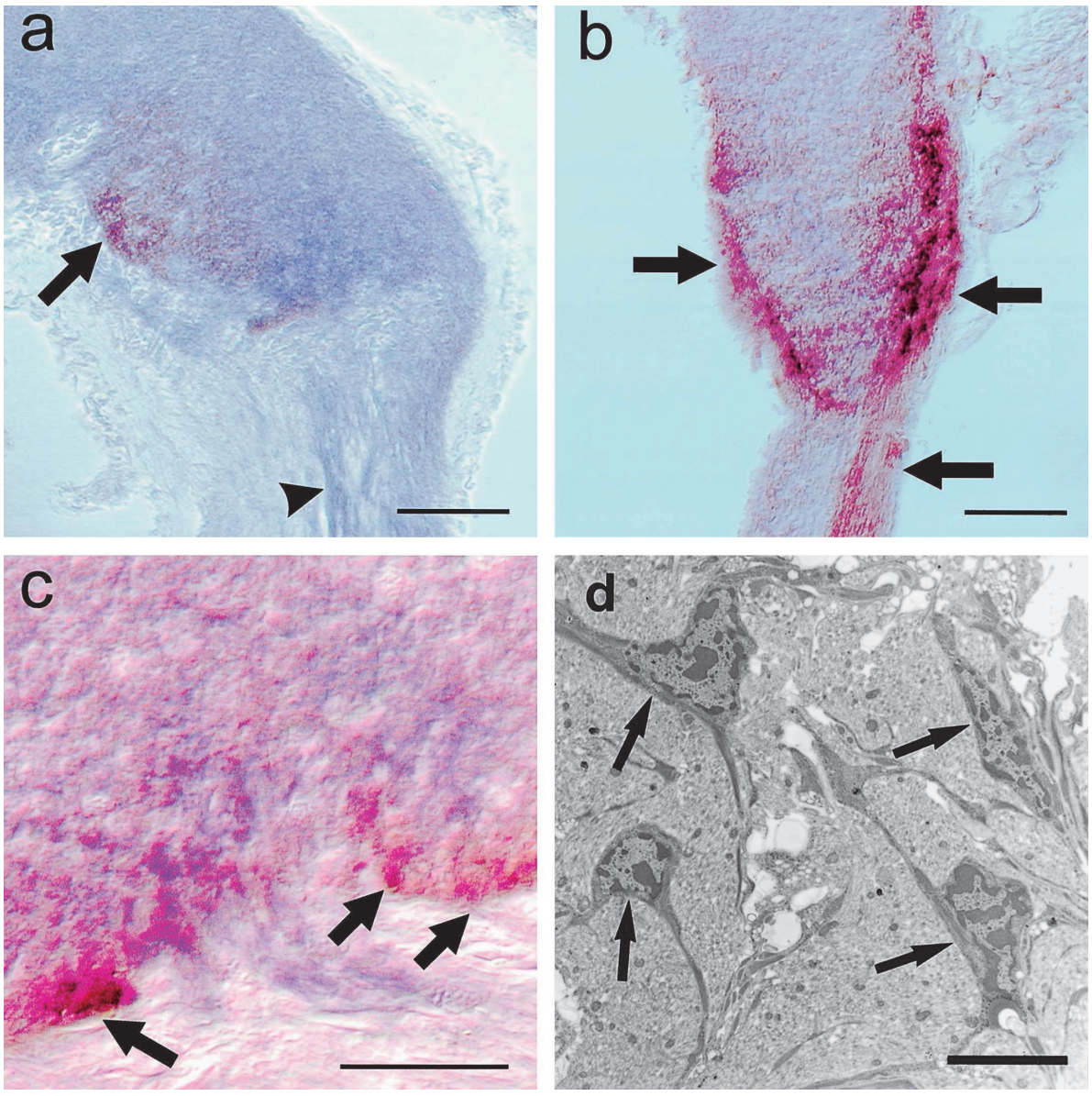

Fig. 3. Double staining for NADPH diaphorase histochemistry and cyclic GMP-like immunohistochemistry in superior and inferior tentacles viewed from the ventral side. Note that NADPH-d signals and cGMP-like immunoreactive signals are deep blue and brown, respectively, and that there were no differences in the staining pattern between the superior and inferior tentacles. (a) A superior tentacle in a cryostat-section preparation. Arrowhead points to NADPH-d stained fibers in the tentacular nerves (TN), which projected to the procerebral lobe. Arrow points to a cGMP-like immunoreactive region in the tentacular ganglion (TG). Scale bar, 150 μm. A; anterior, P; posterior, L; left, R; right. (b) An inferior tentacle in a cryostat-section preparation. Arrows indicate cGMP-like immunoreactive fibers, which projected to the procerebral lobe through the TG and TN as well. Scale bar, 150 μm. (c) A superior tentacle in a cryostat-section preparation. Arrows indicate cGMP-like immunoreactive cells at the boundary between the TG and TN. The NADPH-d stained neuropil passed among these cells. Scale bar, 20 μm. (d) Electron micrograph for the TG in a superior tentacle. Arrows show glia-like cells. Scale bar, 3 μm.

neuropil passed among the cGMP-like immunoreactive cells that were located at the boundary between the tentacular ganglia and the tentacular nerves (Fig. 3c). These cGMP-like immunoreactive cells were identified as glia-like cells by electron microscopy (Fig. 3d).

NADPH diaphorase histochemistry and cyclic GMP-like immunohistochemistry in the central nervous system

First, we examined the NADPH-d reactivity in the CNS. Positively stained cell bodies were found in the major cell body regions in all the central ganglia, including the procerebral lobes (Fig. 4a). The NADPH-d reactive fibers were found consistently in some specific connectives (Fig. 4a). In particular, the fibers in the neuropil regions of the procerebral lobes were strongly reactive. The internal mass neuropil in the procerebral lobes exhibited by far the most intense NADPH-d reactivity of any region of the CNS (Fig. 4b). The terminal mass, which contains neurites of the procerebral

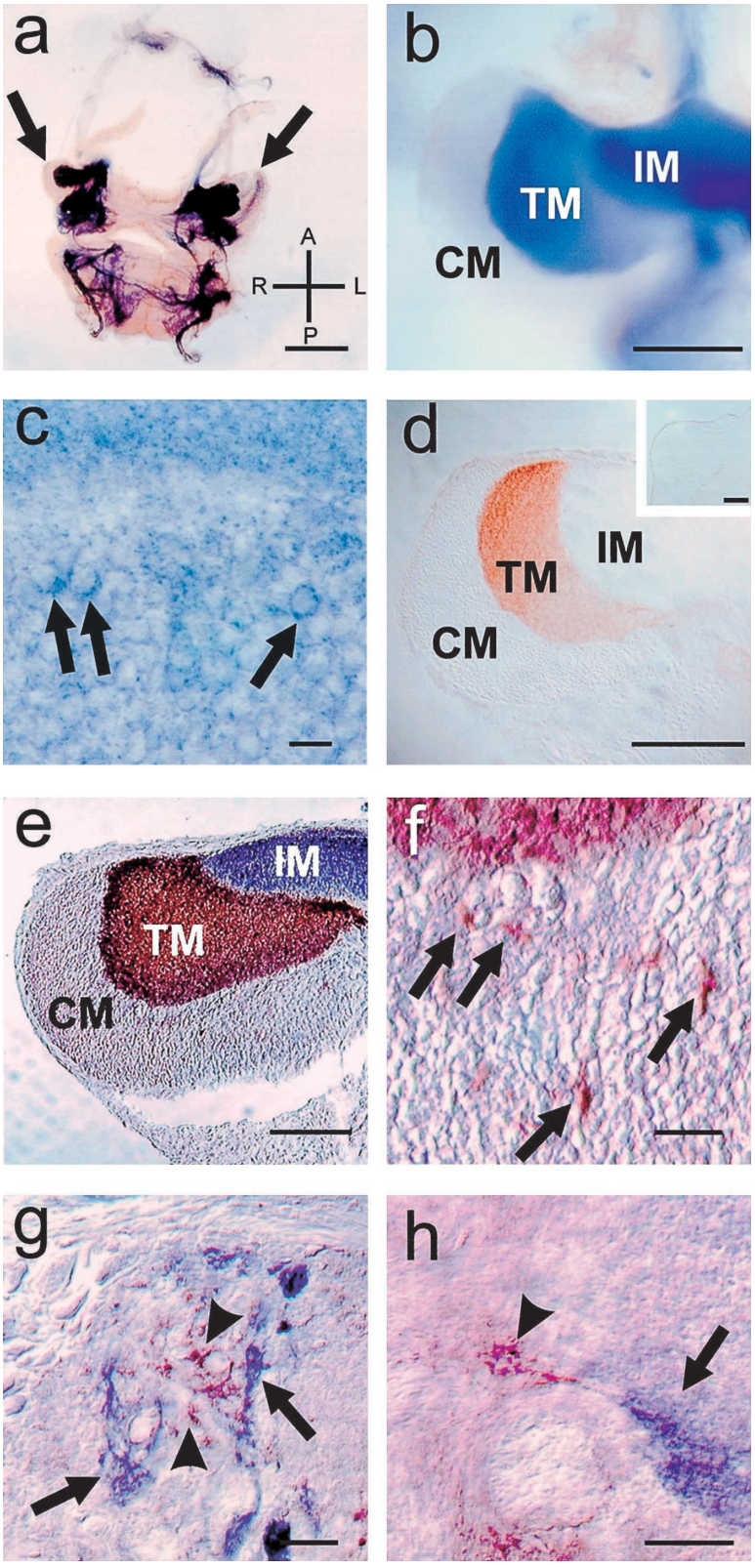

Fig. 4. NADPH diaphorase histochemistry and cyclic GMP-like immunohistochemistry in central nervous system viewed from the ventral side. (a) NADPH-d histochemistry in a whole mount preparation. The procerebral lobes are indicated by a pair of arrows. Scale bar, 300 μm. A; anterior, P; posterior, L; left, R; right. (b) A magnified view of the right procerebral lobe in the whole mount preparation by NADPH-d histochemistry. IM; internal mass, TM; terminal mass, CM; cell mass. Scale bar, 150 μm. (c) CM of the procerebral lobe in a cryostat-section preparation by NADPH-d histochemistry. Arrows indicate NADPH-d stained cells, which are considered to be nonbursting cells. Scale bar, 10 μm. (d) cGMP-like immunohistochemistry of the procerebral lobe in a cryostat-section preparation. Inset shows a control preparation without application of IBMX and SNP. Scale bars, 150 μm. (e) Double staining for NADPH-d histochemistry and cGMP-like immunohistochemistry in the procerebral lobe in a cryostat-section preparation. The IM had NADPH-d reactivity only. The TM and CM had both NADPH-d reactivity and cGMP-like immunoreactivity. Scale bar, 100 μm. (f) CM in a cryostat-section preparation by double staining. Arrows indicate cGMP-like immunoreactive cells. Scale bar, 20 μm. (g) Double staining in the visceral ganglion of a cryostat-section preparation. Arrows indicate NADPH-d stained fibers. Arrowheads indicate cGMP-like immunoreactive cells and fibers. NADPH-d reactive fibers are located near the cGMP positive cells and fibers. Scale bar, 50 μm. (h) Double staining in the cerebral ganglion of a cryostat-section preparation. Arrow points to NADPH-d stained neuropil region; arrowhead points to a cGMP-like immunoreactive cell. Scale bar, 30 μm.

neurons and afferents from olfactory receptors located in the superior and inferior tentacles, also exhibited strong NADPH-d reactivity (Fig. 4b). Tracts of NADPH-d reactive fibers extended between the terminal mass and the cell mass of the procerebral lobes, and some punctate staining was observed in the periphery of many cell bodies in the cell mass (Fig. 4c). The NADPH-d reactive cell bodies in the cell mass were more frequently observed in the basal and mid-

dle regions than in the apical region (data not shown).

Second, we used an immunohistochemical technique for detection of cGMP to determine which regions in the CNS are affected by NO. In the procerebral lobes, the terminal mass was strongly immunoreactive and some cells in the cell mass were slightly stained, whereas no staining was observed in the internal mass (Fig. 4d). When we did not apply IBMX and SNP, or when we excluded the cGMP antibody from the preparations, no detectable staining of cGMP was observed (Fig. 4d).

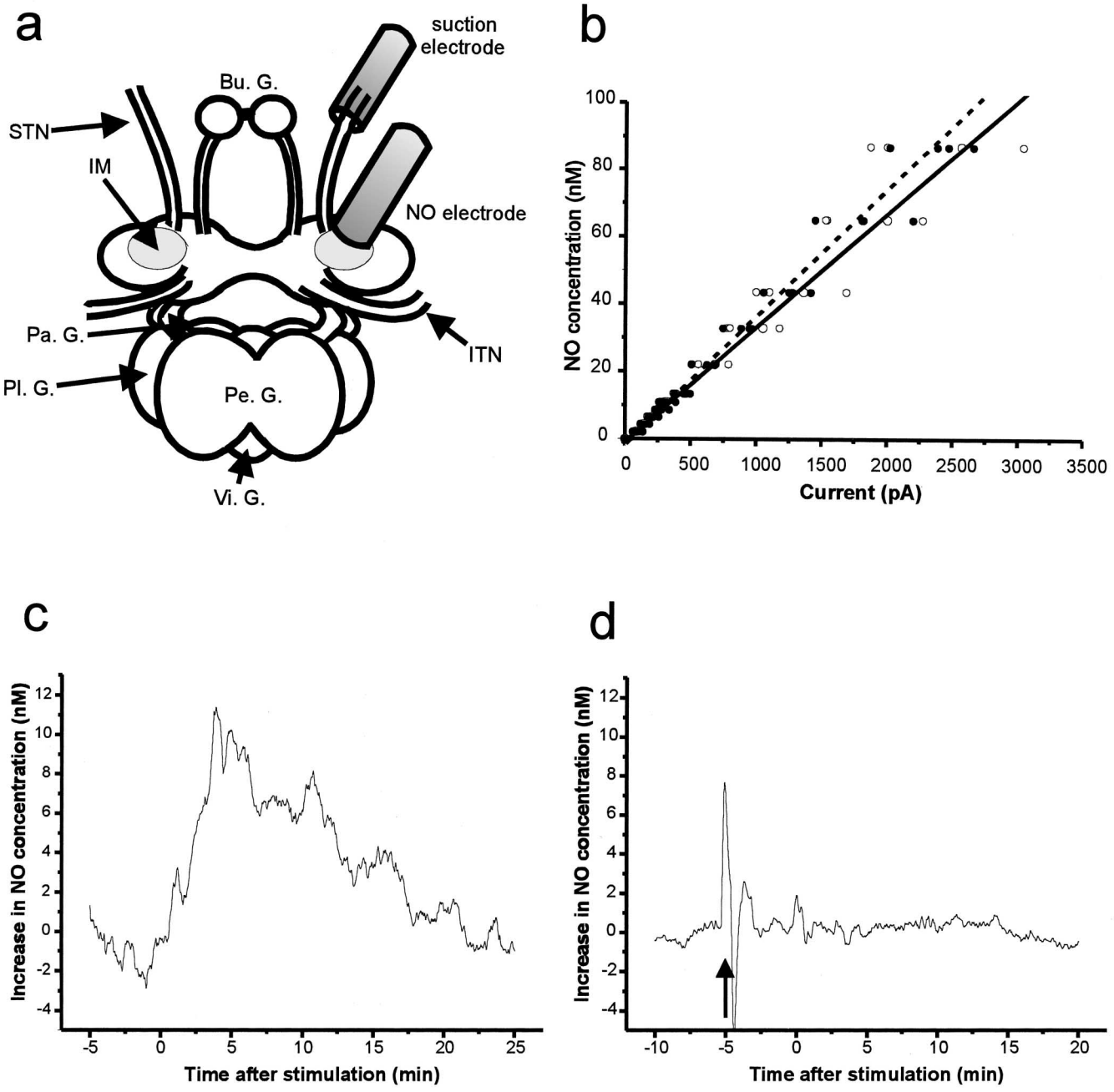

Fig. 5. Nitric oxide measurement around procerebral lobes. (a) Diagram of the preparation of *L. marginatus* and electrodes. The NO electrode was placed on the ventral surface of internal mass (IM). The superior tentacular nerve (STN) end was drawn into the tip of suction electrode to stimulate it. Saline was perfused onto the IM, and PTIO was applied onto the IM by a pipette. Bu. G.; buccal ganglion, Pe. G.; pedal ganglion, Pl. G.; pleural ganglion, Pa. G.; parietal ganglion, and Vi. G.; visceral ganglion, ITN; inferior tentacular nerve. (b) Calibration of the NO meter in acidic condition. Open circles and a solid line represent the data recorded by an NO electrode before experiments; closed circles and a broken line represent the data after experiments (n = 4 each). Note that there were no significant differences between these two calibration lines (two-factor factorial ANOVA). (c) A typical NO response to electric stimulation to the STN. (d) Effect of an NO scavenger, PTIO, on the NO response. Application of PTIO consistently suppressed the NO increases by the STN electric stimulation. Arrow points to the timing of PTIO application.

Third, to analyze the relationship between NO-generative cells and NO-responsive cells, we performed double-staining experiments. Cryostat sections were processed for cGMP-like immunohistochemistry with subsequent NADPH-d histochemistry. In the procerebral lobes, the internal mass was stained by only NADPH-d histochemistry, whereas the terminal mass and the cell mass were stained by both NADPH-d histochemistry and cGMP-like immunohistochemistry (Fig. 4e). Some cells in the cell mass had intense cGMP-like immunoreactivity (Fig. 4f), and these cells were found to be different from the NADPH-d reactive cells by careful observations of double-stained and single-stained preparations. The finding that the NADPH-d reactive cells were different from the cGMP-like immunoreactive ones was also observed in other ganglia. For example, in the cerebral ganglia except the procerebral lobes and in the visceral ganglia, the NADPH-d reactive regions including cell bodies and fibers were adjacent to those showing cGMP-like immunoreactivity but they were completely different (Fig. 4g, h).

Nitric oxide measurement around the procerebral lobes

Because we found that the internal mass had the most intense NADPH-d reactivity (Fig. 4b), we decided to place an NO electrode on the ventral surface of the internal mass to measure the NO responses induced by electrical stimulation of the superior tentacular nerve (Fig. 5a). We paid special attention to the NO calibration, and therefore the NO electrode was calibrated by the chemical titration method before and after each experiment (Fig. 5b). There were no significant differences between the calibration curves before and after experiments (n = 4 each, two-factor factorial ANOVA). The electrical stimulation of the superior tentacular nerve evoked a significant and slow increase in NO concentration around the internal mass (Fig. 5c). The NO response reached a peak 1-5 min after the electrical stimulation, and decreased to the basal level within 20-30 min after the stimulation. The estimated mean peak of NO concentration was 4.8 ± 1.7 nM (mean $\pm$ SEM, n = 7 different preparations). To remove NO in the recording dish, PTIO (NO scavenger) was administered in *Limax* saline. The increase in NO concentration, which was elicited by the electrical stimulation of the superior tentacular nerve, was consistently suppressed by PTIO (Fig. 5d). The NO electrode was confirmed not to be sensitive to NO_2^-, NO_3^-, dopamine, acetylcholine, serotonin, PTIO, or pH changes (pH 4.0, 7.0, 9.0) (data not shown).

DISCUSSION

In the present study, we stained the tentacles and CNS of *L. marginatus* by NADPH-d histochemistry and NO-induced cGMP-like immunohistochemistry to examine the distribution of NO-generative cells and NO-responsive cells, respectively. Our results showed that these two kinds of cells and fibers were localized adjacent to each other in the olfactory system, suggesting the involvement of NO/cGMP pathways in slug olfactory processing.

In the tentacles, some NADPH-d reactive cells appeared to be sensory cells underneath the sensory epithelia and the interneurons between the sensory epithelia and the tentacular ganglia (Fig. 1c-e), whereas cGMP-like immunoreactive cells were all interneurons (Fig. 2b, c). Because the distance between the sensory neurons and interneurons (tens of micrometer) is small enough for rapid diffusion of NO *in vivo* (Sadamoto *et al*., 1998; Philippides *et al*., 2000), our results suggest that NO generation from the sensory neurons and interneurons can increase the cGMP concentration in the adjacent interneurons. From our preliminary experiments with γ-aminobutyric acid (GABA) immunohistochemistry, some interneurons in the tentacles were found to contain GABA, similar to GABAergic cells observed in mouse olfactory bulb (Kishimoto *et al*., 1993). The relation between NO-generative neurons and GABAergic ones will be examined in *Limax* tentacles in future work. Because the collar cells showed NADPH-d reactivity (Fig. 1f), they may be involved in NO generation as well as in hormone secretion. In the tentacular ganglia, the NADPH-d reactivity was very intense (Figs. 1a, b, 3a, b, c), and the cGMP-like immunoreactive cells and fibers (Figs. 2d, e, f, 3a, b, c) were adjacent to, but different from, these NADPH-d reactive regions. In the tentacular nerves as well, the cGMP-like immunoreactive fibers were adjacent to the NADPH-d reactive regions (Fig. 3a, b, c). These results suggest that cGMP as well as NO is responsible for the procerebral lobe responses to inputs from the tentacular nerves.

We should also note that NO can modulate cyclic nucleotide-gated channels directly (Broillet and Firestein, 1996, 1997) or may affect receptor adaptation (Breer and Shepherd, 1993). Therefore, NO produced by sensory neurons underneath the sensory epithelia and by interneurons between the sensory epithelia and the tentacular ganglia (Fig. 1b-d) may directly influence ion channels of the olfactory neurons in slugs. NO also affects growth and migration of neurons and glial cells (Cramer and Sur, 1999; Renteria and Constantine-Paton, 1999; Van Wagenen and Rehder, 1999; Chen *et al*., 2000). Several types of cells including glial cells and receptor cells are continuously generated in the snail tentacles (Chase and Rieling, 1986), and therefore the procerebral lobes continually receive new input fibers (Zakharov *et al*., 1998). By observing ultrathin sections, we also found single cell bodies that contained two nuclei in the central regions of neuropil of tentacular ganglia (data not shown). Because the whole neuropil of the tentacular ganglia showed strong NADPH-d reactivity (Fig. 1a, b), these dividing cells can be influenced by NO. Therefore, NO may play a role in the processes required to integrate these new synapses into the existing circuits in the procerebral lobes and the tentacular ganglia. The role of NO and cGMP in glial cells (Fig. 3c, d) is one of the liveliest topics in neurobiology (Willmott *et al*., 2000).

Both NADPH-d reactivity and cGMP-like immunoreactivity were observed in the terminal mass and the cell mass in the procerebral lobes (Fig. 4b, d, e), whereas only the

NADPH-d staining was observed in the internal mass (Fig. 4b, e). The result that the procerebral lobes were stained well by NADPH-d histochemistry is in good agreement with observations in *L. maximus* (Gelperin, 1994; Gelperin *et al*., 2000). Because the tentacular nerves project only to the terminal mass (Kawahara *et al*., 1997; Watanabe *et al*., 1998), olfactory information transmitted from the tentacles is certainly modulated by NO/cGMP interaction in the olfactory central organ. In addition, the internal mass was strongly stained by NADPH-d histochemistry (Fig. 4b). Because the input pathway from the tentacles runs over the internal mass to terminate at the terminal mass (Kawahara *et al*., 1997), NO signals from the tentacles may be strengthened in the internal mass.

In the cell mass, we note three previous results and one new one: (1) NADPH-d immunoreactive cells are most likely to be nonbursting cells (Gelperin *et al*., 2000); (2) the inhibitory postsynaptic potential (IPSP) in the nonbursting cells is considered to be driven by multiple spikes from the bursting cells (Kleinfeld *et al*., 1994); (3) exogenous NO application induced an increase in the neural oscillatory frequency recorded in the procerebral lobes (Gelperin *et al*., 2000); and (4) both NADPH-d reactive cells and cGMP-like immunoreactive cells were found in the cell mass, and the cGMP-like immunoreactive cells appeared to be bursting cells because of their size and population. These results suggest that cGMP concentration in the bursting cells of the cell mass is increased by NO generated from nonbursting cells and that cGMP-mediated responses play a role in an increase in the neural oscillatory frequency, even though we should still examine other possibilities, for example NO generated from nonbursting cells regulates the activity in nonbursting cells or bursting cells without cGMP cascade.

Taken together, the NADPH-d reactive fibers and the cGMP-like immunoreactive ones in the terminal mass are expected to be the projections of nonbursting cells and the afferents from tentacular nerves, respectively. However, the staining pattern in the cell bodies and projections from the same cells is not usually consistent (e.g. in Kenyon cells in the mushroom body of honeybee; Müller, 1996). We therefore cannot rule out a possibility that the projections of nonbursting cells in the terminal mass are cGMP-like immunoreactive.

The results that the NADPH-d regions were surrounded by NO-induced cGMP-like immunoreactive cells and fibers in the cerebral ganglia and the visceral ganglia as well (Fig. 4g, h) indicate that NO/cGMP pathways are also involved in other brain functions. The observation of whole mount preparations in which the connectives were stained by NADPH-d histochemistry (Fig. 4a), as similarly observed in *Helix* (Cooke, 1994; Sánchez-Alvarez *et al*., 1994), indicates that the regions receiving output from the procerebral lobes may also employ NO/cGMP pathways.

We finally addressed the question: Do NO-generative regions stained by NADPH-d histochemistry release NO (Fig. 5)? We found an NO increase to a concentration of about 5 nM was recorded adjacent to the procerebral lobe after electrical stimulation of the superior tentacular nerve. The validity of the NO measurement methods was confirmed from electrode calibrations described in Materials and Methods and Results. The recorded value of the NO increase suggests that binding of nanomolar concentrations of NO to the prosthetic heme group activates soluble guanylyl cyclase.

In the slug olfactory system, the present results suggest that NO generated from the NO-generative cells by stimulation of an odor input pathway can increase the intracellular cGMP concentration in some of the cells and fibers adjacent to the NO-generative regions. Using this knowledge, we will next investigate the localization of soluble guanylyl cyclase and effects of cGMP on neural oscillations and odor learning.

ACKNOWLEDGMENTS

We thank Dr. De Vente (Rijksuniversiteit Limburg, The Netherlands) for his generous gift of the anti-cGMP antibody and thank World Precision Instruments Japan for providing us with the NO meter. We are grateful to Dr. Oka (Keio University, Japan) for his recommendation to perform cGMP immunohistochemistry. This work was supported in part by Grants-in-Aid from the Ministry of Education, Culture, Sports, Science and Technology of Japan and by grants from Yamada Science Foundation and Itoh Science Foundation to E.I. and by Research Fellowship (No. 05725) of the Japan Society for the Promotion of Science for Young Scientists to I.I.

REFERENCES

Aonuma H, Nagayama T, Takahata M (2000) Modulatory effects of nitric oxide on synaptic depression in the crayfish neuromuscular system. J Exp Biol 203: 3595-3602

Aonuma H, Newland PL (2001) Opposing actions of nitric oxide on synaptic inputs of identified interneurones in the central nervous system of the crayfish. J Exp Biol 204: 1319–1332

Askew SC, Butler AR, Flitney FW, Kemp GD, Megson IL (1995) Chemical mechanisms underlying the vasodilator and platelet anti-aggregating properties of *S*-nitroso-*N*-acetyl-DL-penicillamine and *S*-nitrosoglutathione. Bioorg Med Chem 3: 1–9

Bicker G (2001) Sources and targets of nitric oxide signalling in insect nervous systems. Cell Tissue Res 303: 137–146

Bicker G, Schmachtenberg O, De Vente J (1996) The nitric oxide/cyclic GMP messenger system in olfactory pathways of the locust brain. Eur J Neurosci 8: 2635–2643

Bicker G, Schmachtenberg O, De Vente J (1997) Geometric considerations of nitric oxide-cyclic GMP signalling in the glomerular neuropil of the locust antennal lobe. Proc R Soc Lond B 264: 1177–1181

Bredt DS, Snyder SH (1992) Nitric oxide, a novel neuronal messenger. Neuron 8: 3–11

Breer H, Shepherd GM (1993) Implications of the NO/cGMP system for olfaction. Trends Neurosci 16: 5–9

Broillet MC, Firestein S (1996) Direct activation of the olfactory cyclic nucleotide gated channel through modification of sulfhydryl groups by NO compounds. Neuron 16: 377–385

Broillet MC, Firestein S (1997) Beta subunits of the olfactory cyclic nucleotide-gated channel form a nitric oxide activated Ca^{2+} channel. Neuron 18: 951–958

Chase R, Rieling J (1986) Autoradiography evidence for receptor

cell renewal in the olfactory epithelium of a snail. Brain Res 384: 232–239
Chen A, Kumar SM, Sahley CL, Muller KJ (2000) Nitric oxide influences injury-induced microglial migration and accumulation in the leech CNS. J Neurosci 20: 1036–1043
Cooke IRC, Edwards SL, Anderson CR (1994) The distribution of NADPH diaphorase activity and immunoreactivity to nitric oxide synthase in the nervous system of the pulmonate mollusc *Helix aspersa*. Cell Tissue Res 277: 565–572
Cooke IRC, Gelperin A (2001) *In vivo* recordings of spontaneous and odor-modulated dynamics in the *Limax* olfactory lobe. J Neurobiol 46: 126–141
Cramer KS, Sur M (1999) The neuronal form of nitric oxide synthase is required for pattern formation by retinal afferents in the ferret lateral geniculate nucleus. Develop Brain Res 116: 79–86
Ermentrout B, Flores J, Gelperin A (1998) Minimal model of oscillations and waves in the *Limax* olfactory lobe with tests of the modelís predictive power. J Neurophysiol 79: 2677–2689
Ermentrout B, Wang JW, Flores J, Gelperin A (2001) Model for olfactory discrimination and learning in *Limax* procerebral incorporating oscillatory dynamics and wave propagation. J Neurophysiol 85: 1444–1452
Garthwaite J, Boulton CL (1995) Nitric oxide signaling in the central nervous system. Annu Rev Physiol 57: 683–706
Gelperin A (1994a) Nitric oxide mediates network oscillations of olfactory interneurons in a terrestrial mollusc. Nature 369: 61–63
Gelperin A (1994b) Nitric oxide, odour processing and plasticity. Nether J Zool 44: 159–169
Gelperin A (1999) Oscillatory dynamics and information processing in olfactory systems. J Exp Biol 202: 1855–1864
Gelperin A, Kleinfeld D, Denk W, Cooke IRC (1996) Oscillations and gaseous oxides in invertebrate olfaction. J Neurobiol 30: 110–122
Gelperin A, Flores J, Raccuia-Behling F, Cooke IRC (2000) Nitric oxide and carbon monoxide modulate oscillations of olfactory interneurons in a terrestrial mollusk. J Neurophysiol 83: 116–127
Gelperin A, Kao JPY, Cooke IRC (2001) Gaseous oxides and olfactory computation. Amer Zool 41: 332–345
Gervais R, Kleinfeld D, Delaney KR, Gelperin A (1996) Central and reflex neuronal responses elicited by odor in a terrestrial mollusk. J Neurophysiol 76: 1327–1339
Hatakeyama D, Ito I, Ito E (2001) Complement receptor 3-like immunoreactivity in the superior and interior tentacles of terrestrial slug, *Limax marginatus*. Zool Sci 18: 5–10
Hildebrand JG, Shepherd GM (1997) Mechanisms of olfactory discrimination: converging evidence for common principles across phyla. Annu Rev Neurosci 20: 595–631
Ito I, Kimura T, Suzuki H, Sekiguchi T, Ito E (1999) Effects of electrical stimulation of the tentacular digits of a slug upon the frequency of electrical oscillations in the procerebral lobe. Brain Res 815: 121–125
Ito I, Nakamura H, Kimura T, Suzuki H, Sekiguchi T, Kawabata K, Ito E (2000) Neuronal compounds of the superior and inferior tentacles in the terrestrial slug, *Limax marginatus*. Neurosci Res 37: 191–200
Ito I, Kimura T, Ito E (2001) Odor responses and spontaneous oscillatory activity in tentacular nerves of the terrestrial slug, *Limax marginatus*. Neurosci Lett 304: 145–148
Kawahara S, Toda S, Suzuki Y, Watanabe S, Kirino Y (1997) Comparative study on neural oscillation in the procerebrum of the terrestrial slugs *Incilaria bilineata* and *Limax marginatus*. J Exp Biol 200: 1851–1861
Kendrick KM, Guevara-Guzman R, Zorrilla J, Hinton MR, Broad KD, Mimmack M, Ohkura S (1997) Formation of olfactory memories mediated by nitric oxide. Nature 388: 670–674
Kishimoto J, Keverne EB, Hardwick J, Emson PC (1993) Localization of nitric oxide synthase in the mouse olfactory and vomeronasal system: a histochemical, immunological and in situ hybridization study. Eur J Neurosci 5: 1684–1694
Kleinfeld D, Delaney KR, Fee MS, Flores JA, Tank DW, Gelperin A (1994) Dynamics of propagating waves in the olfactory network of a terrestrial mollusk: an electrical and optical study. J Neurophysiol 72: 1402–1419
Kobayashi S, Ogawa H, Fujito Y, Ito E (2000a) Nitric oxide suppresses fictive feeding response in *Lymnaea stagnalis*. Neurosci Lett 285: 209–212
Kobayashi S, Sadamoto H, Ogawa H, Kitamura Y, Oka K, Tanishita K, Ito E (2000b) Nitric oxide generation around buccal ganglia accompanying feeding behavior in the pond snail, *Lymnaea stagnalis*. Neurosci Res 38: 27–34
Koh HY, Jacklet JW (1999) Nitric oxide stimulates cGMP production and mimics synaptic responses in metacerebral neurons of *Aplysia*. J Neurosci 19: 3818–3826
Marletta MA, Yoon PS, Iyengar R, Leaf CD, Wishnok JS (1988) Macrophage oxidation of L-arginine to nitrite and nitrate: nitric oxide is an intermediate. Biochemistry 27: 8706–8711
Moroz LL (2001) Gaseous transmission across time and species. Amer Zool 41: 304–320
Müller U (1996) Inhibition of nitric oxide synthase impairs a distinct form of long-term memory in the honeybee, *Apis mellifera*. Neuron 16: 541–549
Müller U, Hildebrandt H (1995) The nitric oxide/cGMP system in the antennal lobe of *Apis mellifera* is implicated in integrative processing of chemosensory stimuli. Eur J Neurosci 7: 2240–2248
Okere CO, Kaba H, Higuchi T (1996) Formation of an olfactory recognition memory in mice: reassessment of the role of nitric oxide. Neuroscience 71: 349–354
Ott SR, Jones IW, Burrows M, Elphick MR (2000) Sensory afferents and motor neurons as targets for nitric oxide in the locust. J Comp Neurol 422: 521–532
Philippides A, Husbands P, Oíshea M (2000) Four-dimensional neuronal signaling by nitric oxide: a computational analysis. J Neurosci 20: 1199–1207
Renteria RC, Constantine-Paton M (1999) Nitric oxide in the retinotectal system: a signal but not a retrograde messenger during map refinement and segregation. J Neurosci 19: 7066–7076
Robertson JD, Bonaventura J, Kohm AP (1994) Nitric oxide is required for tactile learning in *Octopus vulgaris*. Proc R Soc Lond B 256: 269–273
Robertson JD, Bonaventura J, Kohm A (1995) Nitric oxide synthase inhibition blocks octopus touch learning without producing sensory or motor dysfunction. Proc R Soc Lond B 261: 167–172
SadamotoH, Hatakeyama D, Kojima S, Fujito Y, Ito E (1998) Histochemical study on the relation between NO-generative neurons and central circuitry for feeding in the pond snail, *Lymnaea stagnalis*. Neurosci Res 32: 57–63
Sánchez-Alvarez M, Leon-Olea M, Talavera E, Pellicer F, Sánchez-Islas E, Martínez-Lorenzana G (1994) Distribution of NADPH-diaphorase in the perioesophageal ganglia of the snail, *Helix aspersa.* Neurosci Lett 169: 51–55
Tanaka J, Markerink van Ittersum M, Steinbusch HWM, De Vent J (1997) Nitric oxide-mediated cGMP synthesis in oligodendrocytes in the developing rat brain. Glia 19: 286–297
Teyke T (1996) Nitric oxide, but not serotonin, is involved in acquisition of food-attraction conditioning in the snail *Helix pomatia*. Neurosci Lett 206: 29–32
Teyke T, Gelperin A (1999) Olfactory oscillations augment odor discrimination not odor identification by *Limax* CNS. NeuroReport 10: 1061–1068
Teyke T, Wang JW, Gelperin A (1999) Lateralized memory storage and crossed inhibition during odor processing by *Limax*. J Comp Physiol A 186: 269–278

Van Wagenen S, Rehder V (1999) Regulation of neuronal growth cone filopodia by nitric oxide. J Neurobiol 39: 168–185

Wang JW, Denk W, Flores J, Gelperin A (2001) Initiation and propagation of calcium-dependent action potentials in a coupled network of olfactory interneurons. J Neurophysiol 85: 977–985

Watanabe S, Kawahara S, Kirino Y (1998) Morphological characterization of the bursting and nonbursting neurons in the olfactory centre of the terrestrial slug *Limax marginatus.* J Exp Biol 201: 925–930

Weyrich AS, Ma X-L, Buerke M, Murohara T, Armstead VE, Lefer AM, Nicolas JM, Thomas AP, Lefer DJ, Vinten-Johansen J (1994) Physiological concentrations of nitric oxide do not elicit an acute negative inotropic effect in unstimulated cardiac muscle. Circ Res 75: 692–700

Willmott NJ, Wong K, Strong AJ (2000) A fundamental role for the nitric oxide-G-kinase signaling pathway in mediating intercellular Ca^{2+} waves in glia. J Neurosci 20: 1767–1779

Zakharov IS, Hayes NL, Ierusalimsky VN, Nowakowski RS, Balaban PM (1998) Postembryonic neurogenesis in the procerebrum of the terrestrial snail, *Helix lucorum* L. J Neurobiol 35: 271–276

(Received October 11, 2001/ Accepted November 10, 2001)